

## Relativistic Resonances in Combined Magnetic and Laser Fields

R. E. Wagner, Q. Su, and R. Grobe

*Intense Laser Physics Theory Unit and Department of Physics, Illinois State University, Normal, Illinois 61790-4560*  
(Received 4 August 1999)

We propose a mechanism for experimental investigation of relativistic effects in the laser-atom interaction with moderate (nonrelativistic) laser intensities that involves placing the system in a static magnetic field parallel to the laser's magnetic-field component. The resonantly induced relativistic motion of the atomic electron leads to a variety of novel phenomena: a relativistic dephasing leading to a ringlike spatial probability density, a counterintuitive window of relativistically enhanced motion, and a sequence of sawtooth-shaped resonances that may increase the harmonic generation.

PACS numbers: 32.80.Rm

Recently ultraintense lasers with intensities up to  $10^{20}$  W/cm<sup>2</sup> have been introduced to study the dynamical properties of electrons that are moving close to the speed of light. One of the practical motivations to study the interaction dynamics is the prospect of producing highly coherent, high-frequency radiation. While high-order harmonics may be produced in very intense laser fields due to bound-free atomic transitions, ionization is one of the main factors limiting the efficient production of the harmonic signals because of the decreasing cross section for electron rescattering with the nuclear core [1–3]. It is thus important to find effective ways to increase the efficiency of harmonic production in lasers with intensities so high that the unwanted ionization can be reduced, and at the same time the nonlinearity due to the relativistic motion can be exploited.

The purpose of this Letter is twofold. First, we propose an experimental scheme to study the relativistic regime of the atom-laser interaction without the need for extremely high-power lasers. This is accomplished by placing the system in a static magnetic field of suitable magnitude and alignment. Conventional lasers are easier to control with respect to intensity, frequency, and pulse duration, and the interaction can be studied over larger ranges of these parameters. Second, we introduce several relativistic phenomena in the electron dynamics that can be observed at moderate laser intensities. These include an enhancement of spatial spreading due to relativistic dephasing perpendicular to the  $B$  field, a window of relativistically enhanced motion, the suppression of spreading due to relativistic kinematic coupling parallel to the  $B$  field, and sawtooth-shaped relativistic resonances.

For geometries that do not permit relativistic resonances, it has been noted that an additional static magnetic field can enhance high-harmonic generation by confining the electron's motion. Using a classical ensemble calculation, Connerade and Keitel [4] showed that the scattered light spectrum also features even harmonics. Zuo *et al.* [5] applied the magnetic field parallel to a two-color laser field and showed that for the nonrelativistic regime the transverse magnetic confinement of the electron's wave packet for a molecular ion  $H_2^+$  reduces the spreading and

increases the high-order harmonic generation efficiency. Salamin and Faisal [6] investigated the suppression of low-order harmonics and enhancement of high-order harmonics in circularly polarized lasers. Very recently, Milosevic and Starace [7] used classical orbit calculations based on the recollision model for the magnetic field case and found field-induced intensity revivals in the spectra.

In each of the above studies the magnetic field was directed perpendicular to that of the laser's magnetic-field component. A relativistic treatment was required only for those cases [4,6] where the laser amplitudes  $E_0$  were so high (with intensities up to  $10^{17}$ – $10^{19}$  W/cm<sup>2</sup>) that the ratio of the (nonrelativistic) quiver velocity  $v_{\text{free}} = qE_0/m\omega_L$  of a free electron in such a field to the speed of light  $c$ ,  $\beta_{\text{free}} = v_{\text{free}}/c$ , was up to  $\beta_{\text{free}} = 3$ . In this case and many other studies in high-field atomic physics, the huge laser intensity that could possibly limit the experimental realization was solely responsible for making the dynamics relativistic. In addition to the benefits due to the confining force by the magnetic field, the collinear configuration with the static and alternating magnetic field introduced in this Letter has the advantage of (1) making possible the use of a peak laser intensity 5 orders in magnitude lower and (2) driving the electron resonantly into relativistic motion. The combined effect will permit a net enhancement of high-harmonic generation by several orders of magnitude.

To be close to experimentally realizable conditions we discuss our results for the CO<sub>2</sub> laser with frequency  $\omega_L = 0.11$  eV and intensity of  $I = 9 \times 10^{13}$  W/cm<sup>2</sup> for which the parameter  $\beta_{\text{free}}$  is only 0.08. But if a static magnetic field of strength close to 10 T is present, the electron's speed can reach up to 80% of the speed of light after only a few laser cycles. This field strength is 10 times weaker than is used in various laboratories [8,9]. Recently, Kudasov *et al.* [10] have produced magnetic-field bursts of  $\mu\text{s}$  duration with an amplitude of 1000 T. Note that these fields are practically constant on the time scale of most laser pulse durations.

To the best of our knowledge, atomic or field-induced resonances have not been used to bring the electron into a relativistic orbit. For an electron in a sufficiently strong

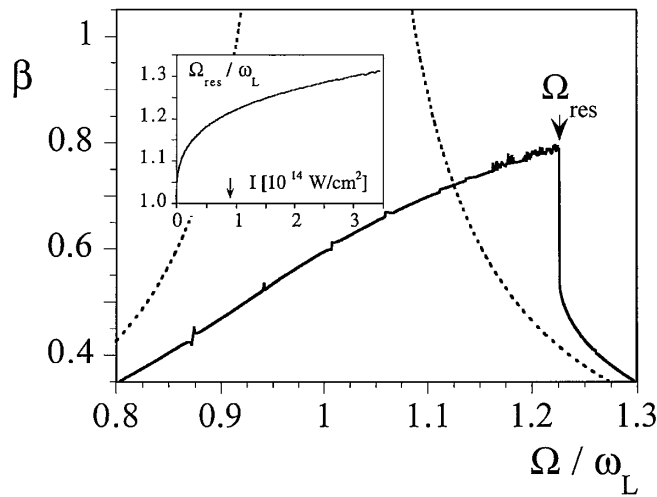


FIG. 1. The maximum speed (in units of  $c$ ) during the interaction as a function of magnetic field  $\Omega = qB_0/mc$  (in units of  $\omega_L$ ) shows a typical sawtooth-shaped resonance. For comparison, the dashed line shows the prediction according to the nonrelativistic theory. The laser parameters were  $I = 9 \times 10^{13} \text{ W/cm}^2$  and  $\omega_L = 0.11 \text{ eV}$ , and the interaction duration was 21.2 ps, long enough to reach the maximum velocity value. The inset shows the location of the sharp edge  $\Omega_{\text{res}}$  as a function of the laser field intensity  $I$ .

magnetic field, however, the velocity can grow to extremely large values until relativistic effects become important and limit the velocity from growing beyond bound. Nonrelativistically, the dynamics of a free electron in combined magnetic and laser fields is equivalent in a rotating frame to a 2D oscillator driven by a bichromatic field. The electron is accelerated by the laser field in phase with the periodic motion induced by the confining static magnetic field until the electron approaches the relativistic speeds.

To study the relativistic dynamics of the electron probability density  $\rho(\mathbf{r}, \mathbf{p}, t)$  in full temporal and spatial resolution the relativistic Liouville equation

$$\frac{\partial \rho(\mathbf{r}, \mathbf{p}, t)}{\partial t} = \left\{ \sqrt{m^2 c^4 + c^2 \left( \mathbf{p} - \frac{q}{c} \mathbf{A}(\mathbf{r}, t) \right)^2} + V(r), \rho(\mathbf{r}, \mathbf{p}, t) \right\}_{\mathbf{r}, \mathbf{p}} \quad (1)$$

is solved numerically. Here  $\{\cdot\}_{\mathbf{r}, \mathbf{p}}$  denotes the Poisson brackets with respect to the six phase space variables, and the vector potential  $\mathbf{A}(\mathbf{r}, t) = -E_0 f(\mathbf{r}, t) c / \omega_L \sin(\omega_L t - \omega_L y / c) \mathbf{e}_x + \frac{1}{2} \mathbf{r} \times (B_0 \mathbf{e}_z)$  represents the linearly polarized laser field with pulse envelope  $f(\mathbf{r}, t)$ , and the static  $B$  field is along the  $z$  direction. Even though none of the phenomena discussed here depends on the details of the initial state,  $\rho(\mathbf{r}, \mathbf{p}, t = 0)$  was chosen to model the hydrogenic ground state for the Coulomb potential  $V(\mathbf{r})$ .

The solution to Eq. (1) leads to an unexpected *relativistically enhanced* response of the atom to the combined laser-magnetic fields. We have monitored the velocity of

the electron during the interaction with the laser pulse, recorded its maximum value  $\beta = v_{\text{max}}/c$ , and then repeated these calculations for various magnetic field “strengths”  $\Omega = qB_0/mc$ . Figure 1 displays  $\beta = \beta(\Omega)$  and shows (1) that if the magnetic field is appropriately tuned,  $B_0 \approx 9.2 \text{ T}$  ( $\Omega \approx 1.2\omega_L$ ), the atom can resonantly absorb an energy of 340 keV ( $\beta \approx 0.8$ ) and (2) a curve that is quite different from the corresponding nonrelativistic (Lorentz-type) resonance profile shown by the dashed line. The drop of the resonance edge denoted by  $\Omega_{\text{res}}$  is extremely sharp, nearly a factor of 2 in this case. This is caused by different types of electron trajectories that are very sensitive to the magnetic-field strength. The location of the edge  $\Omega_{\text{res}}$  increases with the laser intensity as shown in the inset of Fig. 1. For example, for intensities above  $I = 7.6 \times 10^{12} \text{ W/cm}^2$  the  $B$  field needs to be tuned at least 10% above  $mc\omega_L/q$  to generate the edge. At the same time the maximum achievable value of  $\beta$  for  $\Omega = \Omega_{\text{res}}$  (not shown) increases with the laser intensity. We note that in contrast to the simple circular orbit in synchrocyclotrons for which the speed increases practically adiabatically [11], the (continuously) laser driven situation does not permit any helpful closed-form analytical solution. In fact, for certain parameter regimes the motion may even display Kolmogorov-Arnol’d-Moser-type chaos [12].

From a theoretical point of view the most interesting and completely counterintuitive region of “relativistically enhanced” interaction occurs for  $\Omega/\omega_L > 1.12$  in which *the speed is actually greater than that predicted by nonrelativistic theory*. This is quite unusual in that relativistic effects normally lead to a less accelerated and less rapid motion that can be associated with a nonlinear mass increase. For example, at  $\Omega/\omega_L = 1.2$  the electron’s speed is almost twice as large ( $\beta = 0.8$ ) as the corresponding nonrelativistic value ( $\beta \approx 0.4$ ) as indicated by the dashed line. This counterintuitive relativistic effect also has a direct signature in the temporal evolution of the spatial probability.

Figure 2(a) shows the temporal evolution of the spatial probability density  $\rho(x, y, t)$  in the plane perpendicular to the static and alternating magnetic fields. For the first few laser cycles the initially symmetric state (left) follows a spiral-like orbit whose radius oscillates with a frequency related to the “detuning”  $|\Omega - \omega_L|$ . After a few oscillations the state develops a “bananalike” shape (middle) that will finally grow into a ring shaped state displayed in the right figure. The center of this unusually simple and unexpected “ring structure” follows a circular orbit around the nucleus with the period of the laser. The distribution at the origin  $\mathbf{r} = 0$  in the figure reflects the un-ionized electron probability.

To demonstrate that this ring structure is a genuinely relativistic phenomenon, we display in Fig. 2(b) the corresponding spatial distribution obtained from the (nonrelativistic) solution to the Liouville equation for the same

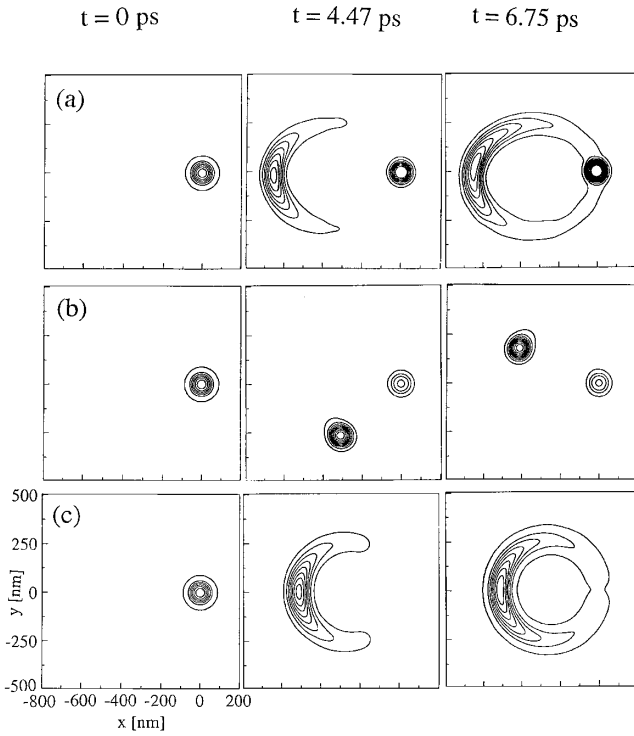


FIG. 2. Snapshots of the spatial probability distribution in the  $(x, y)$  plane  $\rho(x, y, t) = \iint dz d^3 p \rho(\mathbf{r}, \mathbf{p}, t)$  taken at times  $t = 0$ ,  $t = 4.47$  ps (126 laser cycles), and  $t = 6.75$  ps (190 laser cycles). The laser parameters were  $I = 9 \times 10^{13}$  W/cm<sup>2</sup> and  $\omega_L = 0.11$  eV, and the static magnetic-field strength  $B_0 = 9.2$  T, corresponding to  $\Omega = qB_0/mc = 2.2 \times 10^{14}$  Hz. (a) Solution of the relativistic Liouville equation. (b) Solution of the nonrelativistic Liouville equation. (c) Analytical solution based on the relativistic dephasing model, as described below Eq. (2).  $\rho(x, y, t) = \int dz d^3 p d^3 r_0 d^3 p_0 \rho(\mathbf{r}_0, \mathbf{p}_0, t = 0) \delta[\mathbf{r} - \mathbf{r}(\mathbf{r}_0, \mathbf{p}_0, t)] \delta[\mathbf{p} - \mathbf{p}(\mathbf{r}_0, \mathbf{p}_0, t)]$ , where we used the trajectory solutions  $\mathbf{r}(t)$  according to Eq. (2), with a slightly different  $\Omega$  for each initial condition  $\mathbf{r}_0$  and  $\mathbf{p}_0$ .

parameters, which remains much more localized through the entire interaction.

Even though analytical solutions for (1) are unknown, the formation of the ringlike structure may be understood in terms of the relativistic dephasing due to strong velocity dispersion enhanced by the resonance between the magnetic and laser fields. It turns out that the formation of the ring may be reasonably reconstructed from spiral-type (nonclosed) orbits that omit the atomic potential, the magnetic-field component of the laser, relativity, and the smooth laser-turn on:

$$\begin{aligned} x(t) &= x_0 + V_{0x}/\Omega \sin(\Omega t) + V_{0y}/\Omega [\cos(\Omega t) - 1] \\ &\quad - A[\cos(\Omega t) - \cos(\omega_L t)], \\ y(t) &= y_0 + V_{0y}/\Omega \sin(\Omega t) + V_{0x}/\Omega [\cos(\Omega t) - 1] \\ &\quad - A[\sin(\Omega t) - \Omega/\omega_L \sin(\omega_L t)], \end{aligned} \quad (2)$$

with the resonant amplitude  $A = qE_0/[m(\omega_L^2 - \Omega^2)]$ . An ensemble of trajectories obtained using (2) with

various initial values describes the nonrelativistic results for the ionized portion in Fig. 2(b) very well. The natural spreading tendency due to the initial dispersion in velocities is suppressed due to the confining static magnetic field that can lead to a quasiperiodic “breathing” motion [13]. The linearity of the nonrelativistic solution (2) with respect to the initial conditions  $\mathbf{r}_0$  and  $\mathbf{v}_0$  does not permit the nonrelativistic spatial density to spread beyond a maximum value given by the greater of  $2\Delta V_{0x}/\Omega$  and  $\Delta x_0$ .

One would not expect solution (2) to also describe the relativistic ring structure of Fig. 2(a). But if we permit the parameter  $\Omega$  to fluctuate slightly from trajectory to trajectory:  $\Omega \rightarrow \Omega + \Delta\Omega$ , the formation of the rotating ring structure can be qualitatively reproduced as shown in Fig. 2(c). The small dephasing  $\Delta\Omega$ , used to crudely mimic the velocity dependent cyclotron frequencies, was chosen to depend on the initial velocity,  $\Delta\Omega = \Delta\Omega(\mathbf{v}_0)$ . When the interaction time exceeds  $2\pi/\langle\Delta\Omega\rangle$ , where  $\langle\Delta\Omega\rangle$  is an average size of the fluctuation, the angle  $(\Omega + \Delta\Omega)t$  in the oscillating terms is fully randomized, whereas the oscillating terms with the angle  $\omega_L t$  stay coherently in phase. It is quite remarkable that such a simple dephasing mechanism can qualitatively model the relativistic dynamics.

Relativistic effects are also manifest in the radiation that is emitted by the atom [14], which may be of experimental interest. The scattered light spectra detected in the observation direction of the laser’s polarization are displayed in Fig. 3 for three magnetic field strengths around the “relativistic resonance” of Fig. 1. The harmonic energy radiated per unit solid angle per unit frequency along the (normalized) observation direction  $\mathbf{n}$  shown was computed via the radiation (far-field) part of the Lienard-Wiechert potential [15]:

$$\begin{aligned} I_{\mathbf{n}}(\omega) &= \frac{\omega^2}{4\pi^2 c^3} \left| \int \int dt d^3 r \mathbf{n} \right. \\ &\quad \left. \times [\mathbf{n} \times \mathbf{j}(\mathbf{r}, t)] \exp[i\omega(t - \mathbf{n} \cdot \mathbf{r}/c)] \right|^2. \end{aligned} \quad (3)$$

The enhancement of the high-frequency components of the spectrum around the edge  $\Omega_{\text{res}}$  ( $\Omega = 1.17\omega_L$ ) is apparent. From expression (3) we see the harmonic signal is related to the electric current density  $\mathbf{j}$  that depends on the speed  $\beta$  when the light is scattered off. A plot of the scaled speed  $\beta$  at its maximum value as a function of the magnetic field (Fig. 1) clearly displays the  $B$ -field region for which the scattered light spectrum has enhanced high-frequency components. The spectral significance of the counterintuitive relativistically enhanced dynamics is illustrated by a direct comparison with the spectrum obtained from the corresponding nonrelativistic ensemble.

The relativistic enhancement of spatial width due to dephasing is contrasted by the simultaneous suppression of spreading in the  $z$  direction, parallel to the magnetic fields. In the nonrelativistic limit the motion along the  $z$

direction is practically decoupled from the external fields as the coupling through  $V(\mathbf{r})$  is typically small. For large speeds, however, the kinematic coupling in the scalar product  $\mathbf{p}^2$  in Eq. (1) narrows the width of the velocity distribution leading to a reduction of the spatial spreading in the  $z$  direction [16].

Note that due to the nonlinearity induced by the magnetic-field component of the laser there are similar sawtooth-shaped resonances [17] for larger magnetic fields with  $\Omega/\omega_L \approx n$ , each of which can also be exploited to increase the high-frequency scattered light. In contrast to the resonance discussed above, however, the basic aspects of these resonances cannot be modeled with a theory that relies on the dipole approximation.

In summary, we have given several examples of new relativistic phenomena that demonstrate the richness of the relativistic magnetic-laser-atom interaction. This Letter, of course, will raise more questions than it can answer. The spatially localized ringlike electronic structures, which we propose to call cycloatoms, can have average kinetic energies of several hundred keV, and they might have quite interesting optical polarization properties that could be explored using a second probe laser field. Cycloatoms have a submicron extension, and if two cycloatoms collide in

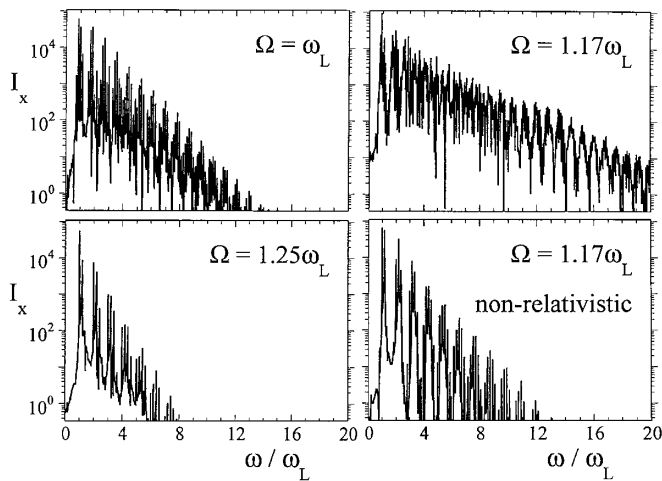


FIG. 3. Relativistic scattered light spectra obtained from the Lienard-Wiechert potential Eq. (3) detected along the laser's polarization direction for three different static magnetic-field strengths  $\Omega$  (in units of  $\omega_L$ ). The  $\text{CO}_2$ -laser field has the frequency  $\omega_L = 0.11$  eV, the intensity  $I = 9 \times 10^{13}$  W/cm<sup>2</sup>, and pulse duration was 1.2 ps. For the lower right graph for  $\Omega = 1.17\omega_L$ , the current density  $\mathbf{j}(\mathbf{r}, t)$  was obtained from the nonrelativistic theory.

a high density target gas novel types of radiation bursts could result from vivid deexcitations that provide new experimental and theoretical challenges. We hope that the opportunity to investigate relativistic cycloatoms at quite moderate laser intensities can help to motivate detailed experimental investigations.

We acknowledge helpful discussions with S.D. Hasani, R.F. Martin, P.J. Peverly, and G.H. Rutherford. This work has been supported by the NSF under Grant No. PHY-9970490. We also acknowledge support from the Research Corporation for Cottrell Science Awards and ISU for URGs. R.E.W. thanks the Illinois State University Undergraduate Honors Program for support of his research work.

- 
- [1] P.B. Corkum, Phys. Rev. Lett. **71**, 1994 (1993).
  - [2] K.C. Kulander, K.J. Schafer, and J.L. Krause, in *Super-Intense Laser-Atom Physics*, edited by B. Piraux, A. L'Huillier, and K. Rzazewski, NATO ASI, Ser. B, Vol. 316 (Plenum, New York, 1993), p. 95.
  - [3] M. Lewenstein, P. Balcou, M. Y. Ivanov, A. L'Huillier, and P.B. Corkum, Phys. Rev. A **49**, 2117 (1994).
  - [4] J.P. Connerade and C.H. Keitel, Phys. Rev. A **53**, 2748 (1996).
  - [5] T. Zuo, A.D. Bandrauk, M.Y. Ivanov, and P.B. Corkum, Phys. Rev. A **51**, 3991 (1995).
  - [6] Y.I. Salamin and F.H.M. Faisal, Phys. Rev. A **58**, 3221 (1998).
  - [7] D.B. Milosevic and A.F. Starace, Phys. Rev. Lett. **82**, 2653 (1999).
  - [8] S. Foner and H.H. Kolm, Rev. Sci. Instrum. **27**, 547 (1956).
  - [9] For a review on nondestructive 100-T magnets, see Phys. Today **51**, No. 10, 21 (1998).
  - [10] Yu.B. Kudasov *et al.*, JETP Lett. **68**, 350 (1998).
  - [11] A.A. Sokolov and I.M. Ternov, *Synchrotron Radiation* (Akademie-Verlag, Berlin, 1968).
  - [12] J.H. Kim and H.W. Lee, Phys. Rev. A **54**, 3461 (1996); R.E. Wagner, P.J. Peverly, Q. Su, and R. Grobe, Phys. Rev. A **61**, 35402 (2000).
  - [13] J.C. Czesznegi, G.H. Rutherford, Q. Su, and R. Grobe, Laser Phys. **9**, 41 (1999).
  - [14] R.E. Wagner, Q. Su, and R. Grobe, Phys. Rev. A **60**, 3233 (1999).
  - [15] J.D. Jackson, *Classical Electrodynamics* (Wiley, New York, 1975).
  - [16] Q. Su, B.A. Smetanko, and R. Grobe, Opt. Exp. **2**, 277 (1998); Laser Phys. **8**, 93 (1998).
  - [17] P.J. Peverly, R.E. Wagner, Q. Su, and R. Grobe, Laser Phys. **10**, 303 (2000).